ISSN 1392–1320 MATERIALS SCIENCE (MEDŽIAGOTYRA). Vol. 30, No. 1. 2024

Engineering in Oxygen-incorporated Monolayer MoS_2 for Efficient Hydrogen Evolution

Jianling MENG [1*], Zheng WEI [2], Shuhua YANG [3], Xiao REN [4]

[1] *Department of Physics, Beijing University of Chemical Technology, Beijing 100029, China*
[2] *School of Materials Science and Engineering, Dalian Jiaotong University, Dalian 116028, China*
[3] *School of Materials Science and Engineering, University of Jinan, Jinan 250022, China*
[4] *Beijing National Laboratory for Molecular Engineering, College of Chemistry and Molecular Engineering, Peking University, Beijing 100871, China*

http://doi.org/10.5755/j02.ms.33985

Received 10 March 2023; accepted 25 July 2023

MoS_2 is a promising alternative to Pt in hydrogen evolution reaction (HER) due to its low cost. To enhance the catalytic properties of the 2H MoS_2 inert basal plane, we propose an approach of employing oxygen incorporated MoS_2 as a catalyst for HER. Different density of oxygen substitution doped monolayer MoS_2 samples ($MoS_{1.51}O_{0.49}$, $MoS_{1.55}O_{0.45}$, $MoS_{1.67}O_{0.33}$) were achieved by chemical vapor deposition method and their catalytic performance were tested. Experimentally, we demonstrate that oxygen substitution can activate the inert basal plane and the catalytic performance is dependent on the oxygen substitution percentage. Also, combining with DFT calculations, we confirm that oxygen substitution act as catalytic sites. Our work provides a strategy for enhancing of monolayer MoS_2 HER activities through in situ substitution doping.

Keywords: monolayer MoS_2, oxygen substitution doping, hydrogen evolution reaction.

1. INTRODUCTION

Electrocatalytic hydrogen evolution reaction (HER) holds tremendous promise as an efficient and green technology to develop a green energy economy. Although excellent HER performance has been reached for platinum and other precious metals, replacing the expensive and rare catalysts with earth-abundant materials still attracts scientists' attention toward making the hydrogen production more economical and competitive. Recently, 2D transition metal dichalcogenides (also known as 2D TMDs) showed their utilization potentiality as cost-effective hydrogen evolution reaction (HER) catalysts in water electrolysis. Among all these 2D TMDs, molybdenum disulfide (MoS_2) has received tremendous attention due to the earth-abundant composition and high activity [1 – 3]. Theoretical work predicted that the basal plane of MoS_2 is catalytically inactive [4] and experimental works demonstrated that edge sites are active sites for hydrogen evolution [5, 6]. To exploit the inert plane, intensive research work has been carried out. One strategy is using 1T metastable phase of MoS_2 due to its metallic property [4]. Another strategy is activating the MoS_2 basal plane through the formation of strained sulfur vacancies [7]. Theoretically, oxygen doping of 2H MoS_2 is a feasible strategy to enhance the catalytic activity. Few works about oxygen doping of MoS_2 nanostructures for efficient electro-catalytic hydrogen generation have been reported [8, 9]. It is interesting that the Levente Tap-asztó group reported the work of monolayer 2H $MoS_{2-x}O_x$ material for HER reaction and demonstrate that oxygen substitution sites act as single-atom reaction centers, substantially increasing the catalytic activity of the entire MoS_2 basal plane for the electrochemical H_2 evolution reaction [10]. The pioneered work experimentally opens a new strategy to manipulate the HER performance of 2H MoS_2 basal plane through oxygen incorporation. Further work on precise control of oxygen substitution percentage in monolayer 2H MoS_2 for HER application is needed.

In this work, we realized the production of $MoS_{2-x}O_x$ material with controllable oxygen substitution percentage ($MoS_{1.51}O_{0.49}$, $MoS_{1.55}O_{0.45}$, $MoS_{1.67}O_{0.33}$) using the method of chemical vapor deposition as reported recently and confirm experimentally that incorporating oxygen into monolayer 2H MoS_2 basal plane can significantly improve the HER performance of MoS_2. $MoS_{2-x}O_x$ materials exhibit a lower overpotential at 10 mA/cm^2 with the increase of oxygen density of substitution and $MoS_{1.51}O_{0.49}$ with the highest density of substitution shows the lowest overpotential 305 mV. Meanwhile, the Tafel slope decrease and the TOF become higher as the density of oxygen substitution increase. In summary, our new discovery is that the HER performance improves as the oxygen substitution percentage increase. The DFT calculations also indicate that oxygen substitution atom in MoS_2 is favorable to the proton adsorption due to the ΔG_H close to zero. ΔG_H is a descriptor for correlating theoretical predictions with experimental measurements of catalytic activity and the optimal value is zero.

* Corresponding author. Tel.: +86-18391862523.
E-mail: *mengjianling@buct.edu.cn* (J. Meng)

2. EXPERIMENTAL DETAILS

2.1. Monolayer $MoS_{2-x}O_x$ growth

The pristine monolayer $MoS_{2-x}O_x$ was grown on c-face sapphire via the chemical vapor deposition (CVD) method, which has been reported elsewhere [11].

2.2. Structural and spectroscopic characterizations

AFM images were characterized by AFM (MultiMode IIId, Veeco Instruments) using tapping mode at room temperature in an ambient atmosphere. The Raman and photoluminescence (PL) spectra were measured by a Horiba Jobin Yvon LabRAM HR-Evolution Raman system with a 532 nm laser (laser power ~10 mW, laser spot size ~1 μm).

2.3. Electrochemical measurement

HER tests were conducted in a three-electrode cell, where the working electrode compartment and counter electrode compartment were separated by an AMI-7001 anion exchange membrane. Working electrodes were fabricated as follows: the as-grown monolayer $MoS_{2-x}O_x$ was spin-coated layer of PMMA (Poly (methyl methacrylate)) (950 5 % in anisole) at 3000 rpm for 60 s and then baked at 180 °C and repeated the spin-coating and baking process. The coated monolayer $MoS_{2-x}O_x$ was etched by 80 °C 2 mol/L KOH deionized water (DI) solution. After several times of DI water rinsing, the coated monolayer $MoS_{2-x}O_x$ films were transferred onto the glassy carbon substrate. Then, the PMMA was dissolved by the lift-off process in acetone for about 10 h. Electrochemical data was recorded by a BioLogic SP-150 potentiostat at room temperature (25 °C). A Pt foil served as a counter electrode and a mercury sulfate (Hg/Hg_2SO_4 in saturated K_2SO_4) was used as a reference electrode. The HER performance was assessed by the cyclic voltammetry (CV) at 10 mV/s in H_2-saturated 0.5 M sulfuric acid (H_2SO_4). The applied potentials were converted to the RHE scale via reference electrode calibration in H_2-saturated 0.5 M H_2SO_4. The potentials were further iR-corrected. R (the uncompensated resistance) was measured by electrochemical impedance spectroscopy (EIS).

3. RESULTS AND DISCUSSION

The monolayer MoS_2 and $MoS_{2-x}O_x$ with controllable oxygen substitution density was deposited by the method which was reported before [11 – 13]. Fig. 1 a shows the typical optical microscope images of large-scale monolayer MoS_2 and $MoS_{2-x}O_x$, which have different color contrast. Fig. 1 b shows the Raman spectra of monolayer MoS_2 and $MoS_{2-x}O_x$ with different oxygen substitution density. The difference (~19.7 cm^{-1}) between E_{2g} (~384.2 cm^{-1}) and A_{1g} (~403.9 cm^{-1}) modes indicates that the thickness of MoS_2 is indeed a single layer [14]. Similar to the reported literature [11], E_{2g} and A_{1g} vibration modes of $MoS_{2-x}O_x$ become red and blue shift respectively and the width of both modes become broaden as the oxygen substitution density increases. Meanwhile, the B_{2g} mode (~287 cm^{-1}) is observed in MoS_2 with high oxygen substitution percentage, corresponding to the vibration modes of Mo-O bonds. It is also noticed that the shoulder peak of A_{1g} modes of all samples is observed, which is the fingerprint of a sapphire substrate. To characterize the composition of $MoS_{2-x}O_x$ quantitatively, the photoluminescence (PL) of monolayer MoS_2 and $MoS_{2-x}O_x$ with different oxygen density is shown in Fig. 1 b. The optical bandgap decreases from 1.881 eV, 1.880 eV, 1.852 eV to PL quench as oxygen substitution density increase. Referring to the literature [15], PL spectral shape is the fingerprint of the doping level of MoS_2. So, we compare the PL spectra in Fig. 1 c with our previous work about in situ oxygen doping monolayer MoS_2 and determine the oxygen substitution level as ~0 %, ~16.5 %, 22.5 %, 24.5 % [11]. Therefore, x is ~0.33, 0.45, 0.49 in $MoS_{2-x}O_x$ from low to high oxygen doping density. The AFM images of monolayer MoS_2 and $MoS_{2-x}O_x$ with different oxygen substitution density show no obvious differences which are shown in Fig. 2. The bright spots on the surface may represent the thick MoS_2 nanoparticles. The steps in the AFM images are from the sapphire substrate.

The HER was measured in 0.5 M H_2SO_4 electrolyte. The current density as a function of potential (versus RHE) from 2H MoS_2, $MoS_{1.67}O_{0.33}$, $MoS_{1.55}O_{0.45}$, $MoS_{1.51}O_{0.49}$ along with those from glassy carbon and Pt for comparison, are shown in Fig. 3 a. This current density is calculated using the catalytic active area of 0.1 cm × 0.125 cm.

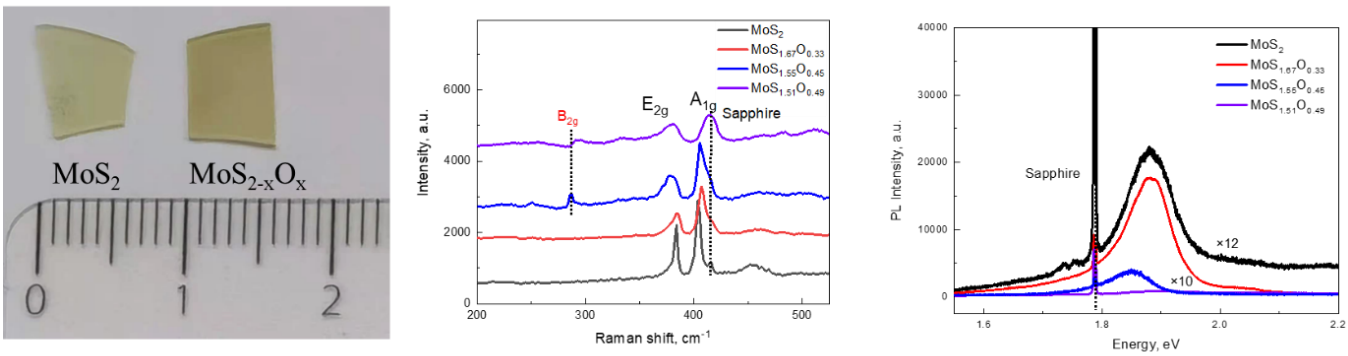

a b c

Fig. 1. a – optical microscope images of MoS_2 and $MoS_{2-x}O_x$; b – Raman spectra; c – PL spectra of monolayer MoS_2 and $MoS_{2-x}O_x$ (x:0.33, 0.45, 0.49)

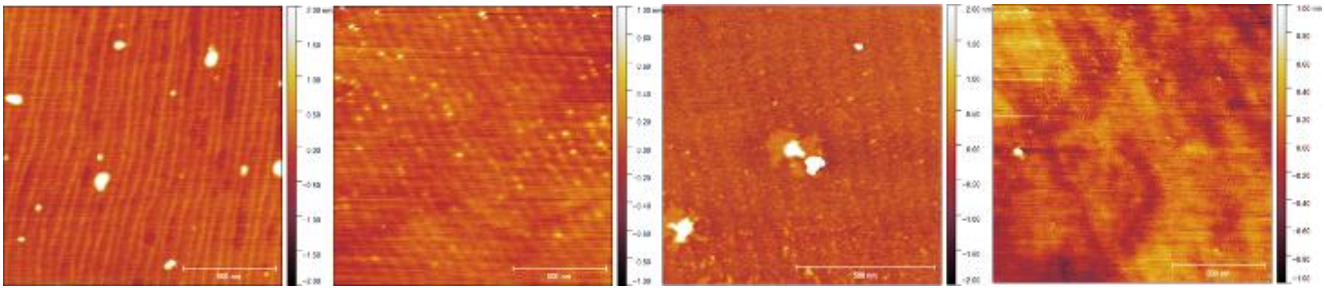

a b c d

Fig. 2. AFM images: a – MoS_2; b – $MoS_{1.67}O_{0.33}$; c – $MoS_{1.55}O_{0.45}$; d – $MoS_{1.51}O_{0.49}$

The Tafel slope is calculated from the linear portion of the Tafel plots, as shown in Fig. 3 c, which can help us to understand the specific reaction mechanism of HER. In the acidic environment, there are three main reaction steps involved in HER, as shown below [14]:

1. Volmer reaction: $H_3O^+ + e^- \rightarrow H_{ads} + H_2O$, Tafel slope value is ~120 mV/dev;
2. Heyrovsky reaction: $H_{ads} + H_3O^+ + e^- \rightarrow H_2 + H_2O$, Tafel slope value is ~40 mV/dev;
3. Tafel reaction: $H_{ads} + H_{ads} \rightarrow H_2$, Tafel slope value is ~30 mV/dev.

The Tafel slopes for 2H MoS_2, $MoS_{1.67}O_{0.33}$, $MoS_{1.55}O_{0.45}$, $MoS_{1.51}O_{0.49}$ are 237 mV/dev, 193 mV/dev, 179 mV/dev, 139 mV/dev respectively, suggesting that adsorption of protons limits the catalytic activity. It is known that proton discharge is the initial step in the acidic solution for the HER and H_3O^+ can be easily adsorbed at Lewis base sites [8]. Here, the O atoms, which replace sulfur atoms in the structure of MoS_2, form a Lewis base on adjacent molybdenum, and this is thought to accelerate the HER in these systems. Meanwhile, the Tafel slope decrease as the density of oxygen substitution increase, indicating the electron transfer speed becomes faster kinetically, which confirms that the HER performance is dependent on the density of oxygen substitution.

In addition to overpotential and Tafel slope, we have also measured the number of hydrogen molecules evolved per second (the turnover frequency, TOF) for the catalysts, as shown in Fig. 3 d. The turnover frequency is calculated using the current density j and the active site density N according to the equation:

$$TOF = \frac{Total\ number\ of\ H_2\ atoms\ per\ second}{Total\ number\ of\ active\ sites\ per\ unit\ area} = \frac{(j/(2*q))}{N}, \quad (1)$$

where $q = 1.6\times10^{-19}$ C is the elementary charge, and 2 accounts for 2 H atoms per H_2 molecule. To calculate the turnover frequency per surface Mo atom (TOF_{Mo}), the Mo atom density (N_{Mo}) is estimated to be about 1×10^{15} cm^{-2} from the MoS_2 lattice constant ~3.2 Å [16]. It is found that TOF for the $MoS_{1.51}O_{0.49}$ is the highest and MoS_2 is the lowest. As the density of oxygen substitution increase, the TOF becomes higher.

To explain the mechanism of enhancement of HER properties through oxygen incorporation of monolayer MoS_2, we calculate the free energy of adsorption of hydrogen on the catalyst surface using first principles calculations implemented in Quantum open-source Package for Research in Electronic Structure, Simulation, and Optimization (ESPRESSO) [17 – 19]. Electron-electron exchange correlations are treated by the local density approximation (LDA) and electron-ion interactions are treated by projector augmented wave (PAW). To ensure the convergence of calculation, the cutoff energy is set to be 65 Ry and the force on each atom is less than 0.04 eV/Å. A vacuum space of 15 Å is adopted to prevent interlayer interactions. The geometric structures are shown in the inset of Fig. 4. The monolayer MoS_2 is modelled by 3×3 atom supercells. MoS_2 with a low density of oxygen substitution is approximately modelled by replacing an S atom by O atom in 3×3 atom supercells and MoS_2 with a high density of oxygen substitution is modelled by replacing an S atom by O atom in 2×2 atom supercells for simplification [20].

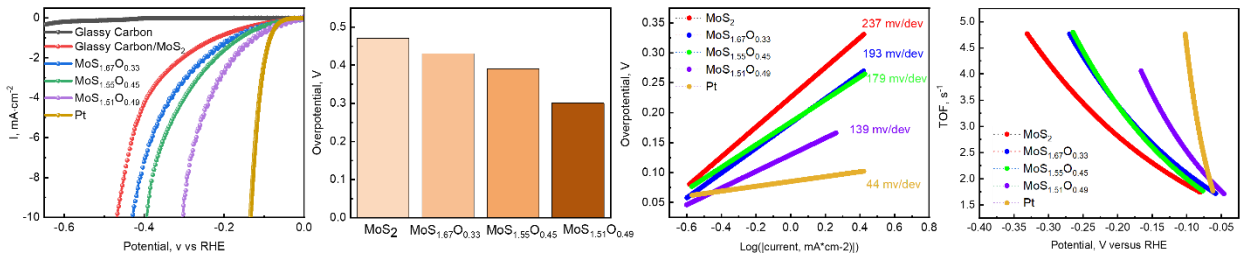

a b c d

Fig. 3. a – linear sweep voltammograms for the glassy carbon substrate, Pt electrode, as-transferred MoS_2, as-transferred $MoS_{1.67}O_{0.33}$, as-transferred $MoS_{1.55}O_{0.45}$, as-transferred $MoS_{1.51}O_{0.49}$; b – corresponding histogram of overpotential vs. RHE at 10 mA/cm^2 current density of the linear sweep voltammograms curves in Fig 3 a; c – corresponding Tafel plots of the linear sweep voltammograms curves in Fig. 3a; d – corresponding turnover frequency per surface Mo atom (TOF_{Mo}) of samples in Fig. 3 a

The O atom doping concentration is 5.6 % and 12.5 %, defined by the number of O atoms divided by the number of S atoms for MoS_2 with low and high density of oxygen substitution respectively. The convergence threshold of self-consistency is set at 1e-10 Ry. The Monkhorst-Pack k-point sampling is set as 1×1×1, 4×4×1, 1×1×1 for structures of $MoS_{2-x}O_x$ (x = 0.00, 0.11, 0.25) respectively. The lattice constant of the optimized geometry structure is 3.12 Å, which is close to the experimental value of 0.32 nm [22]. The hydrogen adsorption free energy (ΔG_H) of $MoS_{2-x}O_x$ (x = 0.00, 0.11, 0.25) is shown in Fig. 4. The hydrogen adsorption free energy was calculated at zero potential and PH=0 as

$$\Delta G_H = \Delta E_H + \Delta E_{ZPE} - T\Delta S\ , \qquad (2)$$

where ΔE_H is the hydrogen adsorption energy; ΔE_{ZPE} is the difference in zero-point energy; T is the temperature (300 K) and ΔS is the difference in entropy between H that is adsorbed and in the gas phase at 1.01E5 pa.

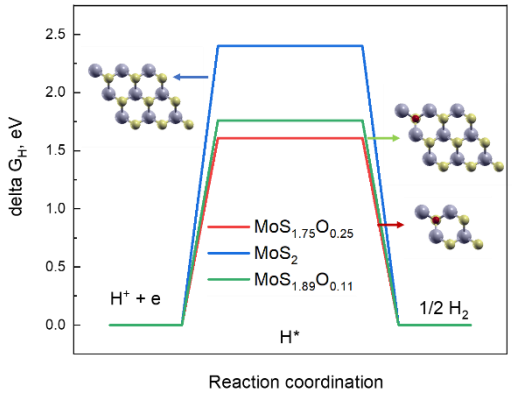

Fig. 4. The free-energy diagram for hydrogen evolution for MoS_2, MoS_2 with low density of oxygen substitution and MoS_2 with high density of oxygen substitution at standard conditions (1 bar of H_2 and PH = 0 at 300 K). The inset shows geometries for monolayer MoS_2, MoS_2 with a low density of oxygen substitution and MoS_2 with a high density of oxygen substitution. The light purple, yellow, red balls are Mo, S and O atoms respectively

For MoS_2, ΔG_H is ~2.3 eV, indicating that the pure MoS_2 is inert in HER activity [21]. It is noted that we use the 3×3 supercell structure as a pure MoS_2 model for greater accuracy and the H atom adsorbs on the S atom [20]. For $MoS_{1.75}O_{0.25}$ and $MoS_{1.89}O_{0.11}$, we calculate ΔG_H using the optimized model of H atom adsorbing on the O atom. The lower ΔG_H value indicates the enhancement of active sites through oxygen substitutions [22]. And ΔG_H value decreases with the density of oxygen substitution increase. Experimentally, $MoS_{1.51}O_{0.49}$ exhibit higher current density than $MoS_{1.67}O_{0.33}$, $MoS_{1.55}O_{0.45}$ and MoS_2 during HER activity. Thus, our work gives an insight into the method of substitution doping to achieve improved performance of MoS_2 catalyst.

4. CONCLUSIONS

In summary, we have introduced a practical method to activate the catalytic performance of MoS_2 by employing oxygen substitution doping. As the density of oxygen substitution increase, the catalytic performance becomes better. The $MoS_{1.51}O_{0.49}$ material exhibits a current density of 10 mA/cm^2 at an overpotential of 305 mV while MoS_2 shows a current density of 10 mA/cm^2 at an overpotential of 469 mV. The DFT calculations demonstrate that the oxygen substitution can decrease the hydrogen adsorption free energy, which acts as catalytic active sites.

Acknowledgments

This research was funded by National Natural Science Foundation of China, grant number No.12104281, No. 52202202 and No.12204084.

REFERENCES

1. **Hu, C., Jiang, Z.Z., Zhou, W.D., Guo, M.M., Yu, T., Luo, X.F., Yuan, C.L.** Wafer-Scale Sulfur Vacancy-Rich Monolayer MoS_2 for Massive Hydrogen Production *Journal of Physical Chemistry Letters* 10 (16) 2019: pp. 4763 – 4768. https://doi.org/10.1021/acs.jpclett.9b01399
2. **Kong, D.S., Wang, H.T., Cha, J.J., Pasta, M., Koski, K.J., Yao, J., Cui, Y.** Synthesis of MoS_2 and $MoSe_2$ Films with Vertically Aligned Layers *Nano Letters* 13 (3) 2013: pp. 1341 – 1347. https://doi.org/10.1021/nl400258t
3. **Benck, J.D., Hellstern, T.R., Kibsgaard, J., Chakthranont, P., Jaramillo, T.F.** Catalyzing the Hydrogen Evolution Reaction (HER) with Molybdenum Sulfide Nanomaterials *ACS Catalysis* 4 (11) 2014: pp. 3957 – 3971. https://doi.org/10.1021/cs500923c
4. **Voiry, D., Salehi, M., Silva, R., Fujita, T., Chen, M. W., Asefa, T., Shenoy, V.B., Eda, G., Chhowalla, M.** Conducting MoS_2 Nanosheets as Catalysts for Hydrogen Evolution Reaction *Nano Letters* 13 (12) 2013: pp. 6222 – 6227. https://doi.org/10.1021/nl403661s
5. **Hinnemann, B., Moses, P.G., Bonde, J., Jørgensen, K.P., Nielsen, J.H., Horch, S., Chorkendorff, I., Nørskov, J.K.** Biomimetic Hydrogen Evolution: MoS_2 Nanoparticles as Catalyst for Hydrogen Evolution *Journal of the American Chemical Society* 127 (15) 2005: pp. 5308 – 5309. https://doi.org/10.1021/ja0504690
6. **Tsai, C., Li, H., Park, S., Park, J., Han, H.S., Nørskov, J.K., Zheng, X., Abild-Pedersen, F.** Electrochemical Generation of Sulfur Vacancies in the Basal Plane of MoS_2 for Hydrogen Evolution *Nature Communications* 8 (1) 2017: pp. 15113. https://doi.org/10.1038/ncomms15113
7. **Li, H., Tsai, C., Koh, A.L., Cai, L.L., Contryman, A.W., Fragapane, A.H., Zhao, J.H., Han, H.S., Manoharan, H.C., Abild-Pedersen, F., Norskov, J.K., Zheng, X.L.** Activating and Optimizing MoS_2 Basal Planes for Hydrogen Evolution Through the Formation of Strained Sulphur Vacancies *Nature Materials* 15 (3) 2016: pp. 48. https://doi.org/10.1038/nmat4465
8. **Peng, J., Yu, X.P., Meng, Y., Tan, H.T., Song, P., Liu, Z., Yan, Q.Y.** Oxygen Doped MoS_2 Quantum Dots for Efficient Electrocatalytic Hydrogen Generation *Journal of Chemical Physics* 152 (13) 2020: pp. 134704. https://doi.org/10.1063/1.5142204
9. **Xie, J.F., Zhang, J.J., Li, S., Grote, F., Zhang, X.D., Zhang, H., Wang, R.X., Lei, Y., Pan, B.C., Xie, Y.** Controllable Disorder Engineering in Oxygen-Incorporated MoS_2 Ultrathin Nanosheets for Efficient Hydrogen Evolution

Journal of the American Chemical Society 135 (47) 2013: pp. 17881 – 17888. https://doi.org/10.1021/ja408329q

10. **Peto, J., Ollar, T., Vancso, P., Popov, Z.I., Magda, G.Z., Dobrik, G., Hwang, C.Y., Sorokin, P.B., Tapaszto, L.** Spontaneous Doping of the Basal Plane of MoS_2 Single Layers Through Oxygen Substitution under Ambient Conditions *Nature Chemistry* 10 (12) 2018: pp. 1246 – 1251. https://doi.org/10.1038/s41557-018-0136-2
11. **Tang, J., Wei, Z., Wang, Q.Q., Wang, Y., Han, B., Li, X.M., Huang, B.Y., Liao, M.Z., Liu, J.Y., Li, N., Zhao, Y.C., Shen, C., Guo, Y.T., Bai, X.D., Gao, P., Yang, W., Chen, L., Wu, K.H., Yang, R., Shi, D.X., Zhang, G.Y.** In Situ Oxygen Doping of Monolayer MoS_2 for Novel Electronics *Small* 16 (42) 2020: pp. 2004276. https://doi.org/10.1002/smll.202004276
12. **Wei, Z., Tang, J., Li, X.Y., Chi, Z., Wang, Y., Wang, Q.Q., Han, B., Li, ., Huang, B.Y., Li, J.W., Yu, H., Yuan, J.H., Chen, H.L., Sun, J.T., Chen, L., Wu, K.H., Gao, P., He, C.L., Yang, W., Shi, D.X., Yang, R., Zhang, G.Y.** Wafer-Scale Oxygen-Doped MoS_2 Monolayer *Small Methods* 5 (6) 2021: pp. 2100091. https://doi.org/10.1002/smtd.202100091
13. **Yu, H., Liao, M.Z., Zhao, W.J., Liu, G.D., Zhou, X.J., Wei, Z., Xu, X.Z., Liu, K.H., Hu, Z.H., Deng, K., Zhou, S.Y., Shi, J.A., Gu, L., Shen, C., Zhang, T.T., Du, L.J., Xie, L., Zhu, J.Q., Chen, W., Yang, R., Shi, D.X., Zhang, G.Y.** Wafer-Scale Growth and Transfer of Highly-Oriented Monolayer MoS_2 Continuous Films *ACS Nano* 11 (12) 2017: pp. 12001 – 12007. https://doi.org/10.1021/acsnano.7b03819
14. **Lee, C., Yan, H., Brus, L.E., Heinz, T.F., Hone, J., Ryu, S.** Anomalous Lattice Vibrations of Single- and Few-Layer MoS_2 *ACS Nano* 4 (5) 2010: pp. 2695 – 2700. https://doi.org/10.1021/nn1003937
15. **Mouri, S., Miyauchi, Y., Matsuda, K.** Tunable Photoluminescence of Monolayer MoS_2 via Chemical Doping *Nano Letters* 13 (12) 2013: pp. 5944 – 5948. https://doi.org/10.1021/nl403036h
16. **Hinnemann, B., Moses, P.G., Bonde, J., Jørgensen, K.P., Nielsen, J.H., Horch, S., Chor-kendorff, I., Nørskov, J.K.** Biomimetic Hydrogen Evolution: MoS_2 Nanoparticles as Catalyst for Hydrogen Evolution *Journal of the American Chemical Society* 127 (15) 2005: pp. 5308 – 5309. https://doi.org/10.1021/ja0504690
17. **Skulason, E., Karlberg, G., Rossmeisl, J., Bligaard, T., Greeley, J.P., Jonsson, H., Norskov, J.K.** Density Functional Theory Calculations for the Hydrogen Evolution Reaction in an Electrochemical Double Layer on the Pt (111) Electrode *Abstracts of Papers of the American Chemical Society* 9 (25) 2007: pp. 3241 – 3250. https://doi.org/10.1039/B700099E
18. **Giannozzi, P., Andreussi, O., Brumme, T., Bunau, O., Buongiorno Nardelli, M., Calandra, M., Car, R., Cavazzoni, C., Ceresoli, D., Cococcioni, M., Colonna, N., Carnimeo, I., Dal Corso, A., de Gironcoli, S., Delugas, P., DiStasio, R.A., Ferretti, A., Floris, A., Fratesi, G., Fugallo, G., Gebauer, R., Gerstmann, U., Giustino, F., Gorni, T., Jia, J., Kawamura, M., Ko, H.Y., Kokalj, A., Küçükbenli, E., Lazzeri, M., Marsili, M., Marzari, N., Mauri, F., Nguyen, N.L., Nguyen, H.V., Otero-de-la-Roza, A., Paulatto, L., Poncé, S., Rocca, D., Sabatini, R., Santra, B., Schlipf, M., Seitsonen, A.P., Smogunov, A., Timrov, I., Thonhauser, T., Umari, P., Vast, N., Wu, X., Baroni, S.** Advanced Capabilities for Materials Modelling with Quantum ESPRESSO *Journal of Physics: Condensed Matter* 29 (46) 2017: pp. 465901. https://doi.org/10.1088/1361-648X/aa8f79
19. **Giannozzi, P., Baroni, S., Bonini, N., Calandra, M., Car, R., Cavazzoni, C., Ceresoli, D., Chiarotti, G.L., Cococcioni, M., Dabo, I., Dal Corso, A., de Gironcoli, S., Fabris, S., Fratesi, G., Gebauer, R., Gerstmann, U., Gougoussis, C., Kokalj, A., Lazzeri, M., Martin-Samos, L., Marzari, N., Mauri, F., Mazzarello, R., Paolini, S., Pasquarello, A., Paulatto, L., Sbraccia, C., Scandolo, S., Sclauzero, G., Seitsonen, A.P., Smogunov, A., Umari, P., Wentzcovitch, R.M.** Quantum Espresso: a Modular and Open-source Software Project for Quantum Simulations of Materials *Journal of Physics: Condensed Matter* 21 (39) 2009: pp. 395502. https://doi.org/10.1088/0953-8984/21/39/395502
20. **Koh, E.W.K., Chiu, C.H., Lim, Y.K., Zhang, Y.W., Pan, H.** Hydrogen Adsorption on and Diffusion Through Mos_2 Monolayer: First-Principles Study *International Journal of Hydrogen Energy* 37 (19) 2012: pp. 14323 – 14328. https://doi.org/10.1016/j.ijhydene.2012.07.069
21. **Luo, Y.T., Zhang, S.Q., Pan, H.Y., Xiao, S.J., Guo, Z.L., Tang, L., Khan, U., Ding, B.F., Li, M., Cai, Z.Y., Zhao, Y., Lv, W., Feng, Q.L., Zou, X.L., Lin, J.H., Cheng, H.M., Liu, B.L.** Unsaturated Single Atoms on Monolayer Transition Metal Dichalcogenides for Ultrafast Hydrogen Evolution *ACS Nano* 14 (1) 2020: pp. 767 – 776. https://doi.org/10.1021/acsnano.9b07763
22. **Yu, Y., Li, C., Liu, Y., Su, L., Zhang, Y., Cao, L.** Controlled Scalable Synthesis of Uniform, High-Quality Monolayer and Few-layer MoS_2 Films *Scientific Reports* 3 2013: pp. 1866. https://doi.org/10.1038/srep01866